Synthesis and Characterization of Cobalt Cyclidene Complexes with Long Polymethylene Bridges and Their Binding to Small Molecules

Peter S. K. Chia,† Mohamad Masarwa,† P. Richard Warburton,† Wei Wu,† Masaaki Kojima,‡ Dennis Nosco,‡ Nathaniel W. Alcock,§ and Daryle H. Busch*,†

Departments of Chemistry, University of Kansas, Lawrence, Kansas 66045, The Ohio State University, Columbus, Ohio 43210, and The University of Warwick, Coventry CV4 7AL, United Kingdom

Received November 4, 1992

The synthesis of four novel cobalt(II) cyclidene complexes with long polymethylene bridges is described. These complexes have been found to reversibly bind dioxygen in a manner similar to that of their shorter bridged analogs. Dioxygen affinities are reduced for bridge lengths exceeding that of octamethylene, an effect which has been correlated with the width of the cavity surrounding the dioxygen-binding site. Structural effects on small-molecule binding that are associated with the long bridge have been examined by comparison of the X-ray crystal structure of the undecamethylene-bridged cobalt(III) complex with the shorter bridged analogues. Bis(isothiocyanato)(2,3,15,16,17,24-hexamethyl-3,15,19,23,26,30-hexaazabicyclo- [15.7.7]hentriaconta-1,16,18,23,25,30-hexaene-κ^4N)cobalt(III) hexafluorophosphate crystallizes in space group $P2_1$ with a = 13.699(6) Å, b = 9.515(3) Å, c = 14.726(7) Å, and β = 97.40(4)°, and the structure was solved by the heavy-atom method to R = 0.053, R_w = 0.058. The thiocyanate that is coordinated within the cavity is bent through steric interaction with the ligand and has bond lengths and angles closer to those of the externally bound thiocyanate than is true of analogous complexes with shorter bridges. The cavity width of the six-coordinate undecamethylene-bridged cobalt(III) complex is similar to that of the octamethylene-bridged complex, in contradistinction to the previous observation that the widths of vacant cavities decrease as the bridge length increases beyond $(CH_2)_8$. This clearly shows that that the longer bridged complexes are flexible enough to expand their cavities when a small molecule is coordinated to the metal center. The autoxidation of these cobalt(II) complexes has been found to depend on the dioxygen partial pressure and the axial base in a manner analogous to that of the shorter bridged derivatives. However, the rate of autoxidation is significantly greater for the complexes having longer bridges.

Introduction

There has been much interest over the last few decades in producing reversible dioxygen carriers, which mimic the biological dioxygen carriers hemoglobin and myoglobin, and several new families of dioxygen carriers have been developed[1] (see reviews[2]). The cobalt(II) and iron(II) cyclidene complexes are among the best families of dioxygen carriers when judged in terms of dioxygen affinity and resistance to autoxidation, and the cyclidenes currently include the only well-characterized reversible iron(II) dioxygen carriers that do not contain the porphyrin ring.[3] These totally synthetic materials are, therefore, particularly significant in providing a second family of dioxygen carriers that may be compared to the porphyrins. Additional advantages accrue from the ease with which structural variations may be carried out on the ligand, facilitating systematic study of the effects of structural perturbations. The structure of the cyclidene complexes, shown in Figure 1, consists of a saddle-shaped macrocyclic ligand, which forms an intrinsic cavity within which O_2 binds, and a superstruture that bridges the cavity.[3,4] It has previously been shown that dramatic structural changes occur when the length of the polymethylene bridging group exceeds that of octamethylene.

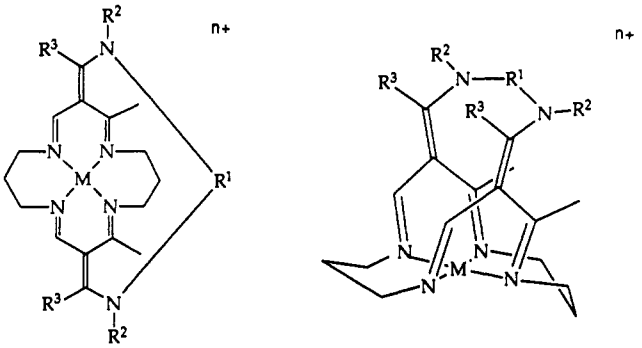

Figure 1. Planar and three-dimensional representations of the cyclidene complexes. These complexes are conveniently denoted as $M(R^3)_2(R^2)_2(R^1)^{2+}$, where M = Ni(II) or Co(II).

† University of Kansas.
‡ The Ohio State University.
§ The University of Warwick.

(1) (a) Goedken, V. L.; Kildahl, N. K.; Busch, D. H. *J. Coord. Chem.* **1977**, *7*, 89. (b) Martell, A. E. In *Oxygen Complexes and Oxygen Activation by Transition Metals*; Martell, A. E., Sawyer, D. T., Eds.; Plenum Press: New York, 1988. (c) Basallotte, M. G.; Martell, A. E. *Inorg. Chem.* **1988**, *27*, 4219. (d) Motekaitis, R. J.; Martell, A. E. *Inorg. Chem.* **1988**, *15*, 1. (e) Kimura, E. J. *J. Coord. Chem.* **1986**, *15*, 1. (f) Delgado, R.; Glowgowski, M. W.; Busch, D. H. *J. Am. Chem. Soc.* **1987**, *109*, 6855. (g) Ramprasad, D.; Lin, W. K.; Goldsby, K. A.; Busch D. H. *J. Am. Chem. Soc.* **1988**, *110*, 1480. (h) Chen, D.; Sun, Y.; Martell, A. E. *Inorg. Chem.* **1989**, *28*, 2647. (i) Ransahoff, S.; Adams, M. T.; Dzugan, S. J.; Busch, D. H. *Inorg. Chem.* **1990**, *29*, 2945. (j) Dzugan, S. J.; Busch, D. H. *Inorg. Chem.* **1990**, *29*, 2528. (k) Lance, K. A.; Goldsby, K. A.; Busch, D. H. *Inorg. Chem.* **1990**, *29*, 4537. (l) Lance, K. A.; Goldsby, K. A.; Busch, D. H. *Inorg. Chem.* **1990**, *29*, 2528. (m) Abushamleh, A. S.; Chmielewski, P. J.; Warburton, P. R.; Morales, L.; Stephenson, N. A.; Busch, D. H. *J. Coord. Chem.* **1991**, *23*, 91. (n) Lance, K. A.; Lin, W. K.; Busch, D. H.; Alcock, N. W. *Acta Crystallogr.* **1991**, *C47*, 1401. (o) Stephenson, N. A.; Dzugan, S. J.; Gallucci, J. C.; Busch, D. H. *J. Chem. Soc., Dalton Trans.* **1991**, 733.

(2) (a) Traylor, T. G.; Traylor, P. S. *Annu. Rev. Biophys. Bioeng.* **1982**, *11*, 105. (b) Collman, J. P.; Halbert, T. R.; Suslick, K. S. In *Metal Ion Activation of Dioxygen*; Spiro, T. G., Ed.; Wiley & Sons: New York, 1980; p 1. (c) Niederhoffer, E. C.; Timmons, J. H.; Martell, A. E. *Chem. Rev.* **1984**, *84*, 137. (d) Smith, T. D.; Pilbrow, J. R. *Coord. Chem. Rev.* **1981**, *39*, 295. (e) Jones, R. D.; Summerville, D. A.; Basolo, F. *Chem. Rev.* **1979**, *79*, 139. (f) McLendon, G.; Martell, A. E. *Coord. Chem. Rev.* **1976**, *19*, 1. (g) Vaska, L. *Acc. Chem. Res.* **1976**, *9*, 175. (h) Basolo, F.; Hoffman, B. M.; Ibers, J. *Acc. Chem. Res.* **1975**, *8*, 384.

(3) Herron, N.; Busch, D. H. *J. Am. Chem. Soc.* **1981**, *103*, 1236. Herron, N.; Cameron, J. H.; Neer, G. L.; Busch, D. H. *J. Am. Chem. Soc.* **1983**, *105*, 298. Herron, N.; Zimmer, L. L.; Grzybowski, J. J.; Olszanski, D. J.; Jackels, S. C.; Callahan, R. W.; Cameron, J. H.; Cristoph, G. G.; Busch, D. H. *J. Am. Chem. Soc.* **1983**, *105*, 6585. Busch, D. H. *Trasfus. del Sangue* **1988**, *33*, 57.

0020-1669/93/1332-2736$04.00/0

The present study is concerned with the influence of these modifications in the ligand structure on the molecular properties of the cobalt(II) complexes, especially their interaction with dioxygen. While substitution of R^3 and R^2 has been shown to affect the electronic properties of the nickel(II) complexes, variation in the length of R^1 has little effect on the nickel(III/II) redox potential for these materials.[5] For the cobalt(II) complexes with $R^3 = R^2 = CH_3$ and $R^1 = (CH_2)_n$, the dioxygen-binding affinity in acetonitrile, containing a large excess of a nitrogenous base such as 1-methylimidazole, systematically increases over 4 orders of magnitude on varying n from 4 to 8.[4a] This dependence on the bridge length has been directly correlated with the width of the cyclidene cavity, within which the dioxygen binds to the metal.[6] Prior to this work, the dependence of bridge conformation on the $(CH_2)_n$ chain length has been examined by ^{13}C NMR and X-ray crystallography for the long-bridged nickel(II) cyclidene complexes.[6c] These studies revealed that the nickel(II) complex with the dodecamethylene bridge exhibited a significantly reduced cavity width, resulting from a change in conformation of the bridge, and consequently, the oxygen affinity of the corresponding cobalt(II) complex is predicted to be significantly lower.[6c,7]

This work describes the synthesis and characterization of cobalt(II) cyclidene complexes with $R^3 = R^2 = CH^3$ and $R^1 = (CH_2)_n$, with n = 9–12, and their reactions with dioxygen. The crystal structure of the bis(isothiocyanate) undecamethylene-bridged cobalt(III) complex has been solved, disclosing the effects on the conformation of the cyclidene ligand of coordination of a small molecule within the cavity. The dioxygen affinities and autoxidation reactions of the long-bridged cobalt(II) complexes are discussed and compared to those of the shorter bridged cobalt(II) cyclidene complexes.

Experimental Section

Solvents were purified according to published methods. 1,10-bis(*p*-tolylsulfonyl)nonane, -decane, -undecane, and -dodecane were prepared as previously described.[6c,8]

Preparation of Nickel(II) Cyclidene Complexes. The nickel(II) Jäger complex was prepared and methylated as previously described with methyl trifluoromethanesulfonate in dichloromethane, to give the methylated Jäger complex, which reacted with methylamine hydrochloride (2 equiv) in methanol containing 2 equiv of triethylamine, to give the unbridged nickel(II) cyclidene complex $Ni(CH_3)_2(CH_3)_2(H)_2^{2+}$ (abbreviations defined in Figure 1).[9]

$Ni(CH_3)_2(CH_3)_2(CH_2)_n(PF_6)_2$ (n = 9–12). The long-bridged nickel(II) cyclidene complexes were prepared as previously described.[6c] After $Ni(CH_3)_2(CH_3)_2(H)_2^{2+}$ was deprotonated in acetonitrile with sodium methoxide, the appropriate α,ω-bistosylated polymethylene diol was added under high-dilution conditions. The product was purified by chromatography and precipitated as the PF_6^- salt, on addition of a methanolic ammonium hexafluorophosphate solution and sufficient ethanol to initiate solid formation. Yields: 40%, n = 9; 27%, n = 10; 40%, n = 11; 40%, n = 12.

Table I. Physical Properties of Long-Polymethylene-Bridged Cobalt(II) Cyclidene Complexes, $[Co(CH_3)_2(CH_3)_2(CH_2)_n](PF_6)_2$ (n = 9–12)

complex	anal., %: C, H, N	mass spect, FAB/NBA: expt (calc)	Co(III/II) $E_{1/2}$, V vs Fc/Fc^+; ΔE_p, mV (CH_2Cl_2)
n = 9	calc: 41.89, 6.06, 10.11	540 CoL (542)	0.22; 80
	expt: 38.55, 5.96, 9.14	686 CoL(PF_6) (687)	
n = 10	calc: 42.61, 6.20, 9.94	554 CoL (556)	0.22; 100
	expt: 41.10, 6.25, 9.60	700 CoL(PF_6) (701)	
n = 11	calc: 43.32, 6.33, 9.78	569 CoL (570)	0.23; 95
	expt: 42.82, 6.27, 10.29	715 CoL(PF6) (715)	
n = 12	calc: 44.00, 6.46, 9.62	583 CoL (584)	0.20; 95
	expt: 43.90, 6.50, 9.80	729 CoL(PF_6) (720)	

Preparation of Cyclidene Ligand Salts. All four cyclidene complexes were demetalated to form the ligand salts by the method applied previously to cyclidene complexes.[5b,9] The corresponding lacunar nickel(II) cyclidene complex was suspended in dry methanol (30 mL) in a flask fitted with inlet and outlet drying tubes. HBr gas was bubbled through the mixture. The nickel(II) complex dissolved, and after another 15 min of bubbling, a green-blue solution was obtained. The solvent was removed, and a yellow-green solid remained. Water (10 mL) was added to dissolve the residue, and ammonium hexafluorophosphate (1 g) in water (10 mL) was added dropwise. The off-white solid was collected and dried in vacuo. The yields were all above 80%, and the salts were used without further characterization.

Preparation of Cobalt(II) Cyclidene Complexes: (2,3,13,14,16,22-Hexamethyl-3,13,17,21,24,28-hexaazabicyclo[13.7.7]nonacosa-1,14,-16,21,23,28-hexaene-κ^4N)cobalt(II) Hexafluorophosphate, $Co(CH_3)_2(CH_3)_2(CH_2)_9(PF_6)_2$; (2,3,14,15,17,23-Hexamethyl-3,14,18,22,25,29-hexaazabicyclo[14.7.7]triaconta-1,15,17,22,24,29-hexaene-κ^4N)cobalt(II) Hexafluorophosphate, $Co(CH_3)_2(CH_3)_2(CH_2)_{10}(PF_6)_2$; (2,3,15,16,-18,24-Hexamethyl-3,15,19,23,26,30-hexaazabicyclo[15.7.7]hentriaconta-1,16,18,23,25,30-hexaene-κ^4N)cobalt(II) Hexafluorophosphate, $Co(CH_3)_2(CH_3)_2(CH_2)_{11}(PF_6)_2$; (2,3,16,17,19,25-Hexamethyl-3,16,-20,24,27,31-hexaazabicyclo[16.7.7]dotriaconta-1,17,19,24,26,31-hexaene-κ^4N)cobalt(II) Hexafluorophosphate, $Co(CH_3)_2(CH_3)_2(CH_2)_{12}(PF_6)_2$. The cobalt(II) cyclidene complexes were all prepared in the same general manner as has been applied to the shorter bridged cobalt(II) cyclidene complexes.[9] In an inert-atmosphere box, the ligand salt (0.5 g assumed to be $L(PF_6)_3$) was slurried in methanol (15–20 mL), and this mixture was heated to boiling. One equivalent of cobalt(II) acetate tetrahydrate and 3 equiv of sodium acetate in boiling methanol (10–15 mL) were added to the ligand slurry. An immediate dark orange-red color developed. The mixture was allowed to reflux for about 20 min. Upon cooling and being stirred for a few hours, the mixture was filtered, and the volume of the filtrate was reduced to yield an orange-red solid. The solid was dissolved in the minimum amount of acetonitrile, the solution was filtered, and ethanol was added. The volume of the solution was reduced, and then more ethanol was added. This procedure was repeated until most of the acetonitrile was removed. At this stage, an orange solid was obtained. This solid was collected and dried under vacuum at room temperature. The complex $Co(CH_3)_2(CH_3)_2(CH_2)_{11}(PF_6)_2$ precipitated from the solution about 4 h after all of the reactants were added. The solid was purified by the same procedure as above. The yields for all of the cobalt(II) complexes were about 40%. The elemental analyses, shown in Table I, were found to be satisfactory. All four of the long-bridged cobalt(II) cyclidene complexes exhibited peaks by FAB/NBA mass spectroscopy that were consistent with the molecular mass minus one and two PF_6^- ions: $CoL(PF_6)$ and CoL. These results are summarized in Table I. ESR spectra of the cobalt(II) complexes and of the dioxygen adducts were found to be similar to related cobalt(II) cyclidene complexes.[4a,10] A detailed investigation of the ESR spectra of the cobalt(II) cylidenes and their dioxygen adducts will be presented elsewhere.[10]

Bis(isothiocyanato)(2,3,15,16,17,24-hexamethyl-3,15,19,23,26,30-hexaazabicyclo[15.7.7]hentriaconta-1,16,18,23,25,30-hexaene-κ^4N)cobalt(III) Hexafluorophosphate, $[Co^{III}(CH_3)_2(CH_3)_2(CH_2)_{11}(NCS)_2](PF_6)$. The cobalt(II) complex $Co^{II}(CH_3)_2(CH_3)_2(CH_2)_{11}^{2+}$ was prepared *in situ* by addition of the ligand salt, dissolved in a mixture of acetonitrile (25 mL) and methanol (15 mL), to a solution of cobalt acetate (0.1469 g) and sodium acetate (0.0484 g) in methanol (50 mL) under nitrogen, to give an immediate orange coloration. A 10-fold excess of sodium

(4) (a) Busch, D. H. In Oxygen Complexes and Oxygen Activation by Transition Metals; Martell, A. E., Sawyer, D. T., Eds.; Plenum Press: New York, 1988. (b) Busch, D. H.; Stephenson, N. A. In *Inclusion Compounds*; Atwood, J., Davies, E., MacNicol, D., Eds.; Oxford University Press: Oxford, U.K., 1991; Vol. 5.
(5) (a) Busch, D. H.; Olszanski, D. J.; Stevens, J. C.; Schammel, W. P.; Kojima, M.; Herron, N.; Zimmer, L. L.; Holter, K.; Mocak, J. *J. Am. Chem. Soc.* **1981**, *103*, 1472. (b) Busch, D. H.; Jackels, S. C.; Callahan, R. C.; Grzybowski, J. J.; Zimmer, L. L.; Kojima, M.; Olszanski, D. J.; Schammel, W. P.; Stevens, J. C.; Holter, K. A.; Mocak, J. *Inorg. Chem.* **1981**, *20*, 2834.
(6) (a) Stevens, J. C.; Busch, D. H. *J. Am. Chem. Soc.* **1980**, *102*, 3285. (b) Goldsby, K. A.; Meade, T. J.; Kojima, M.; Busch, D. H. *Inorg. Chem.* **1985**, *24*, 2588. (c) Alcock, N. W.; Padolik, P. A.; Pike, G. A.; Kojima, M.; Cairns, C. J.; Busch, D. H. *Inorg. Chem.* **1990**, *29*, 2599. (d) Busch, D. H.; Stephenson, N. A. *J. Inclusion Phenom. Mol. Recognit. Chem.* **1989**, *7*, 137.
(7) (a) Alcock, N. W.; Lin, W.-K.; Cairns, C.; Pike, G. A.; Busch, D. H. *J. Am. Chem. Soc.* **1989**, *111*, 6630. (b) Busch, D. H.; Stephenson, N. A. *J. Inclusion Phenom. Mol. Recognit. Chem.* **1989**, *7*, 137.
(8) Marvel, C. S.; Sekera, B. C. *Org. Synth.* **1940**, *20*, 50.
(9) Cairns, C. J.; Busch, D. H. *Inorg. Synth.* **1990**, *27*, 261.
(10) Chmielewski, P.; Busch, D. H.; et al. Manuscript in preparation.

thiocyanate (0.478 g; dissolved in water, 7 mL) was added to the cobalt(II) cyclidene solution, to give a dark red solution. Cerium(IV) ammonium nitrate (0.324 g) in methanol (50 mL) was added, also under nitrogen, and the solution was left to stir under nitrogen overnight. After removal of the solvent, the oily green residue was purified by chromatography on neutral alumina and eluted with acetonitrile. The first red-brown band was collected, solvent volume was reduced, and ammonium hexafluorophosphate (0.29 g) in methanol was added. The solution was reduced in volume on a rotary evaporator with incremental addition of methanol to gradually increase the proportion of methanol, until the solid began to form. After refrigeration overnight, the red-brown crystals were collected by suction filtration, washed with ethanol, and dried in vacuo. The deep red lath crystals were suitable for X-ray study without further recrystallization. The identity of $[Co(CH_3)_2(CH_3)_2(CH_2)_{11}(NCS)_2](PF_6)$ was confirmed by FAB/NBA mass spectroscopy. The predominant peak was observed at m/z 685 consistent with $[Co(CH_3)_2(CH_3)_2(CH_2)_{11}(NCS)_2]^+$, and the next two peaks observed were consistent with the further loss of one and two thiocyanate anions, at m/z 627 $(Co(CH_3)_2(CH_3)_2(CH_2)_{11}(NCS)^+)$ and 568 $(Co(CH_3)_2(CH_3)_2(CH_2)_{11} + H^+)$.

Instrumentation. All inert-atmosphere manipulations were performed in a nitrogen-filled Vacuum Atmospheres Corp. (VAC) glovebox, equipped with a gas circulation and dioxygen removal system, either a VAC MO40-1 or HE-493 dry train. Dioxygen concentrations were maintained below 1 ppm.

UV–visible spectrophotometric studies were conducted using a 1-cm gastight quartz cell, fitted with a gas inlet and a bubbling tube. Spectra were recorded on either a Varian 2300 spectrophotometer or a Hewlett Packard 8452 diode array spectrophotometer, with a 9000 (300) Hewlett Packard Chem Station. The Varian spectrophotometer was connected to an IBM personal computer, which controlled the spectrometer and allowed automated data collection. Both instruments incorporated flow-through temperature-regulated cell holders connected to a Neslab or Fisher Scientific constant-temperature circulation system, giving a temperature precision of ±0.2 °C. Dioxygen/nitrogen gas mixtures were mixed using Tylan FC-260 mass flow controllers.

Electrochemical experiments were performed within the glovebox, using a single-compartment cell. The working electrode was a 3 mm diameter glassy carbon electrode in Kel-F (Bioanalytical Systems), the secondary electrode was a platinum wire, and a silver wire was used for the reference electrode. Potentials were measured versus ferrocene, which was used as an internal standard. The experiments were undertaken using a Princeton Applied Research (PAR) Model 175 programmer and a PAR Model 173 potentiostat, and the output was directly recorded on paper using a Houston Instruments Model 200 X-Y recorder.

Equilibrium constants for the formation of the 1:1 cobalt–dioxygen adducts were determined by monitoring UV–visible changes as a function of a partial pressure of dioxygen[6a] and were fitted, on an IBM Model 80 PS/2 computer, to the Ketelaar equation,[11] using a BASIC program written by Dr. Naidong Ye of this research group.

Kinetic studies on these complexes were performed using the above spectrophotometers, with freshly prepared solutions, and the kinetics parameters were evaluated either by using the Hewlett Packard proprietary software accompanying the HP spectrometer/Chem Station for data collected from this instrument or by using programs written in BASIC by Dr. Naidong Ye of this group.

Infrared spectra were obtained using a Perkin-Elmer Model 1600 FTIR instrument. Samples were examined either as potassium bromide disks or in acetonitrile solution, in which case the background was fresh acetonitrile.

Fast atom bombardment (FAB) mass spectra were obtained on a VG ZAB HS mass spectrometer equipped with a xenon gun. The FAB experiments were performed in a matrix of either a 3:1 mixture of dithiothreitol and dithioerythritol (FAB/MB) or 3-nitrobenzyl alcohol (FAB/NBA).

Elemental analyses were performed either at the University of Kansas or by Galbraith Laboratories Inc., Knoxville, TN.

X-ray Structure Determination. Crystal data are given in Table II. At room temperature, the crystal diffracted weakly and decomposed rapidly in the X-ray beam; therefore, it was held at 220 K with an Oxford Cryosystems Cryostream Cooler. Data were collected with a Siemens R3m four-circle diffractometer in the ω–2θ mode. Maximum 2θ was 50° with scan range ±0.7°(ω) around the $K\alpha_1$–$K\alpha_2$ angles and scan speed 3.5–15°(ω) min^{-1}, depending on the intensity of a 2-s prescan; backgrounds were measured at each end of the scan for one-fourth of the scan time. hkl ranges: 0/11; 0/13 (with some $-k$ data also); -14/14.

Table II. Data Collection and Refinement Details for the X-ray Structural Determination of $[Co(CH_3)_2(CH_3)(CH_2)_{11}(NCS)_2](PF_6)_2$

empirical formula	$CoC_{33}H_{54}N_8S_2PF_6$
fw	830.8
cryst system	monoclinic
space group	$P2_1$
a, Å	13.699(6)
b, Å	9.515(3)
c, Å	14.726(7)
β, deg	97.40(4)
V, Å^3	1903.5
Z	2
dens(calcd), g cm^{-3}	1.45
λ, Å	0.710 69
μ(Mo Kα), mm^{-1}	0.67
no. of unique rflcns	3482
no. of rflcns with $I/\sigma(I) \geq 2.0$	2244
cryst dimens, mm	0.058 × 0.14 × 0.64
R	0.053
T, K	220

Three standard reflections were monitored every 200 reflections and showed no change during data collection. Unit cell dimensions and standard deviations were obtained by a least-squares fit to 15 reflections ($15 < 2\theta < 19°$). The 4276 reflections collected were processed using profile analysis to give 3482 unique reflections ($R_{int} = 0.032$), of which 2244 were considered observed ($I/\sigma(I) \geq 2.0$). These were corrected for Lorentz, polarization, and absorption effects (by the Gaussian method); minimum and maximum transmission factors were 0.91 and 0.96. Crystal dimensions were 0.058 × 0.14 × 0.64 mm.

Systematic reflection conditions $0k0$, $k = 2n$, indicate either space group $P2_1/m$ or $P2_1$. Although molecular mirror symmetry (required for the former) is possible, the intensity statistics indicated the noncentrosymmetric alternative. This was adopted and confirmed when the Patterson solution located Co, P, and two S atoms in an arrangement without a mirror plane. These heavy atoms were located by the Patterson interpretation section of SHELXTL, and the light atoms were then found by successive Fourier syntheses. The high thermal parameters of C(22)–C(24) indicate the presence of some disorder in this part of the polymethylene chain, though no specific partially occupied atomic positions could be located.

Anisotropic thermal parameters were used for all non-H atoms. Hydrogen atoms were given fixed isotropic thermal parameters, $U = 0.08$ Å^2. Those defined by the molecular geometry were inserted at calculated positions and not refined; methyl groups were treated as rigid CH_3 units, with their initial orientation based on a staggered configuration. The absolute structure of the individual crystal chosen was checked by refinement of a $\delta f''$ multiplier. The y-coordinate of the Co atom was fixed to define the origin. Final refinement was on F by least-squares methods refining 474 parameters. Largest positive and negative peaks on a final difference Fourier synthesis were of heights +0.6 and –0.5 e Å^{-3}.

A weighting scheme of the form $w = I/(\sigma^2(F) + gF^2)$ with $g = 0.0012$ was used and shown to be satisfactory by a weight analysis. Final $R = 0.053$, $R_w = 0.058$, and $S = 1.07$; R (all reflections) = 0.103. Maximum shift/error in the final cycle was 0.2. Computing was performed with SHELXTL PLUS (Sheldrick, 1986) on a DEC Microvax-II.[12] Scattering factors were in the analytical form, and anomalous dispersion factors were taken from ref 13. Final atomic coordinates are given in Table III, and selected bond lengths and angles, in Table IV.

Results and Discussion

The characterization of the $Ni^{II}(CH_3)(CH_3)(CH_2)_n^{2+}$ cyclidene complexes with $n = 9$, 10, and 12 has been published previously.[6c] The ligand salts, produced by demetalation of the nickel(II) cyclidene complexes with HBr gas, were not purified, but they gave satisfactory results when used directly in the synthesis of the

(11) Ketelaar, J. A. A; Van de Stolpe, C.; Gouldsmit, A.; Dzcubas, W. *Recl. Trav. Chim. Pays-Bas* **1952**, *71*, 1104.

(12) Sheldrick, G. M. *SHELXTL PLUS User's Manual*; Nicolet: Madison, WI, 1986.

(13) *International Tables for X-Ray Crystallography*; Kynoch Press: Birmingham, U.K., 1974 (present distributor Kluwer Academic Publishers, Dordrecht); Vol. IV.

Table III. Atom Coordinates ($\times 10^4$) and Isotropic Thermal Parameters for $[Co(CH_3)_2(CH_3)(CH_2)_{11}(NCS)_2](PF_6)_2$

atom	x	y	z	U,[a] Å^2
Co(1)	2407.0(8)	00.0	9049.6(8)	27(1)
N(01)	1606(5)	−1360(10)	8378(5)	28(2)
C(01)	1104(6)	−2341(10)	8273(6)	24(2)
S(1)	378(2)	−3653(3)	8073(2)	52(1)
N(02)	3206(6)	1306(10)	9759(6)	36(2)
C(02)	3591(6)	2304(12)	10077(6)	32(2)
S(2)	4127(2)	3719(4)	10479(2)	52(1)
N(1)	3214(5)	140(10)	8058(5)	30(2)
N(2)	3235(6)	−1532(9)	9542(5)	31(2)
N(3)	1563(5)	−120(10)	9999(4)	32(2)
N(4)	1514(6)	1496(9)	8529(5)	30(2)
N(5)	3434(5)	−3767(8)	6720(5)	30(2)
N(6)	−1278(5)	−296(8)	7922(5)	34(2)
C(1)	3563(7)	−950(11)	7665(6)	34(2)
C(2)	4131(8)	−739(12)	6864(7)	51(2)
C(3)	3557(7)	−2301(11)	8065(6)	35(2)
C(4)	3578(6)	−2416(12)	9022(6)	35(2)
C(5)	3447(7)	−1758(12)	10535(6)	40(2)
C(6)	2513(7)	−1837(12)	10989(7)	43(2)
C(7)	2003(7)	−452(11)	10939(6)	34(2)
C(8)	643(6)	−65(12)	9838(6)	35(2)
C(9)	106(6)	346(10)	8987(6)	30(2)
C(10)	566(6)	1396(10)	8472(6)	31(2)
C(11)	−80(6)	2486(11)	7985(7)	42(2)
C(12)	1962(7)	2748(11)	8236(7)	38(2)
C(13)	2575(7)	2398(11)	7460(6)	37(2)
C(14)	3464(7)	1553(11)	7788(7)	36(2)
C(15)	3779(7)	−3538(11)	7589(7)	33(2)
C(16)	4510(7)	−4613(11)	8017(7)	47(2)
C(17)	3875(7)	−4733(11)	6135(6)	41(2)
C(18)	2545(7)	−3036(11)	6273(6)	38(2)
C(19)	1739(8)	−4081(12)	5970(7)	50(2)
C(20)	820(8)	−3366(14)	5538(7)	64(2)
C(21)	−31(9)	−4355(17)	5362(8)	79(3)
C(22)	−947(9)	−3668(26)	4945(12)	161(3)
C(23)	−1752(12)	−3836(30)	5101(12)	242(3)
C(24)	−2431(17)	−3828(21)	5623(16)	246(3)
C(25)	−2926(8)	−2656(16)	5974(8)	70(3)
C(26)	−3181(11)	−2748(16)	6921(9)	90(3)
C(27)	−2496(9)	−2227(12)	7656(8)	58(2)
C(28)	−2314(7)	−671(11)	7668(8)	44(2)
C(29)	−747(7)	−254(13)	7133(6)	45(2)
C(30)	−848(6)	−147(11)	8775(6)	32(2)
C(31)	−1422(7)	−663(12)	9508(7)	45(2)
P(1)	6125(2)	−7638(4)	6378(2)	47(1)
F(1)	4962(5)	−7642(8)	6127(5)	74(2)
F(2)	6076(5)	−6127(8)	6774(5)	75(2)
F(3)	5991(5)	−8289(7)	7343(4)	60(2)
F(4)	7277(4)	−7649(9)	6663(5)	75(2)
F(5)	6138(6)	−9199(8)	6006(4)	80(2)
F(6)	6236(6)	−7015(9)	5420(5)	93(2)

[a] Equivalent isotropic U defined as one-third of the trace of the orthogonalized U_{ij} tensor.

cobalt complexes as described previously for the shorter chain cobalt(II) cyclidene complexes.[9,14] The long-bridged cobalt(II) cyclidene complexes were satisfactorily characterized by elemental analyses and FAB mass spectroscopy, as shown in Table I.

The cobalt(III/II) redox potentials for these complexes in methylene chloride are also shown in Table I. Cyclic voltammograms of the long-bridged cobalt(II) complexes were qualitatively similar to those of the shorter bridged complexes. In a noncoordinating solvent such as methylene chloride, the cobalt(III/II) couple is quasi-reversible. The peak separation is typically larger in methylene chloride than in more highly conductive media due to the larger ohmic drop. The cobalt(III/II) redox potentials are in the region typical for the shorterchained analogues. In acetonitrile or methanol, both coordinating solvents, the cyclic voltammograms of the long-bridged complexes exhibited completely irreversible cobalt(II) oxidation waves (E_p^a = 0.36 V vs Fc/Fc$^+$, $Co(CH_3)_2(CH_3)_2(CH_2)_{12}^{2+}$/MeCN). These results are consistent with the expectation that the large cavities should allow the cobalt(III) form of the complex to become six- coordinate following oxidation whereas, under these conditions, the cobalt(II) cyclidene complexes are invariably five-coordinate. The back sweeps displayed very broad, small, and poorly defined reductive processes, at ca. 0.5 V more negative potential ($E°$(ferrocene/ferrocenium (Fc/Fc$^+$)) = 0.41 V vs NHE[15]). This result is consistent with the reductive process being regulated by a preceding chemical reaction, a so-called CE process.[16] The preceding reaction is presumably the unfavorable formation of the five-coordinate cobalt(III) complex. Otherwise, in their electrochemical behavior, the long-bridged cobalt cyclidene complexes are analogous to the shorter bridged complexes.[17]

The dioxygen-binding properties of the long-bridged cyclidene complexes were determined by the dependence of the UV–visible spectral changes on the partial pressure of dioxygen, as described in the Experimental Section (Figure 2). Experimental conditions involved solutions of the cobalt(II) complex, typically ~10^{-5} M, in acetonitrile, in the presence of an excess of a nitrogenous axial

Table IV

(A) Selected Bond Lengths (Å) for $[Co(CH_3)_2(CH_3)(CH_2)_{11}(NCS)_2](PF_6)_2$

Co(1)–N(01)	1.891(8)	Co(1)–N(02)	1.881(8)
Co(1)–N(1)	1.946(7)	Co(1)–N(2)	1.931(8)
Co(1)–N(3)	1.929(7)	Co(1)–N(4)	1.967(8)
N(01)–C(01)	1.158(13)	C(01)–S(1)	1.601(10)
N(02)–C(02)	1.156(14)	C(02)–S(2)	1.610(11)
N(1)–C(1)	1.308(13)	N(1)–C(14)	1.456(13)
N(2)–C(4)	1.267(13)	N(2)–C(5)	1.468(12)
N(3)–C(7)	1.471(10)	N(3)–C(8)	1.253(11)
N(4)–C(10)	1.294(12)	N(4)–C(12)	1.432(13)
N(5)–C(15)	1.324(12)	N(5)–C(17)	1.444(13)
N(5)–C(18)	1.481(11)	N(6)–C(28)	1.464(12)
N(6)–C(29)	1.449(13)	N(6)–C(30)	1.324(11)
C(1)–C(2)	1.508(15)	C(1)–C(3)	1.415(15)
C(3)–C(4)	1.410(13)	C(3)–C(15)	1.423(14)
C(5)–C(6)	1.520(14)	C(6)–C(7)	1.488(15)
C(8)–C(9)	1.423(12)	C(9)–C(10)	1.447(13)
C(9)–C(30)	1.386(12)	C(10)–C(11)	1.487(13)
C(12)–C(13)	1.538(14)	C(13)–C(14)	1.487(13)

(B) Selected Bond Angles (deg) for $[Co(CH_3)_2(CH_3)(CH_2)_{11}(NCS)_2](PF_6)_2$

N(01)–Co(1)–N(02)	177.7(4)	N(1)–Co(1)–N(4)	92.4(3)
N(3)–Co(1)–N(4)	85.7(3)	Co(1)–N(01)–C(01)	156.4(7)
N(01)–C(01)–S(1)	176.6(8)	Co(1)–N(02)–C(02)	166.0(8)
N(02)–C(02)–S(2)	177.7(9)	Co(1)–N(1)–C(1)	123.6(7)
Co(1)–N(1)–C(14)	116.4(6)	C(1)–N(1)–C(14)	119.9(8)
Co(1)–N(2)–C(4)	121.3(6)	Co(1)–N(2)–C(5)	121.0(7)
C(4)–N(2)–C(5)	117.6(8)	Co(1)–N(3)–C(7)	118.9(5)
Co(1)–N(3)–C(8)	122.8(6)	C(7)–N(3)–C(8)	117.9(7)
Co(1)–N(4)–C(10)	122.7(7)	Co(1)–N(4)–C(12)	116.8(6)
C(10)–N(4)–C(12)	120.5(8)	C(15)–N(5)–C(17)	123.8(7)
C(15)–N(5)–C(18)	121.6(8)	C(17)–N(5)–C(18)	114.6(7)
C(28)–N(6)–C(29)	111.8(7)	C(28)–N(6)–C(30)	124.6(8)
C(29)–N(6)–C(30)	123.3(7)	N(1)–C(1)–C(2)	119.7(9)
N(1)–C(1)–C(3)	120.9(9)	C(2)–C(1)–C(3)	118.6(9)
C(1)–C(3)–C(4)	119.1(9)	C(1)–C(3)–C(15)	122.2(9)
C(4)–C(3)–C(15)	116.8(9)	N(2)–C(4)–C(3)	126.2(10)
N(2)–C(5)–C(6)	112.1(7)	C(5)–C(6)–C(7)	110.5(9)
N(3)–C(7)–C(6)	111.7(8)	N(3)–C(8)–C(9)	124.8(8)
C(8)–C(9)–C(10)	116.1(8)	C(8)–C(9)–C(30)	118.1(8)
C(10)–C(9)–C(30)	125.2(8)	N(4)–C(10)–C(9)	121.2(8)
N(4)–C(10)–C(11)	120.7(9)	C(9)–C(10)–C(11)	117.5(8)
N(4)–C(12)–C(13)	109.9(8)	C(12)–C(13)–C(14)	112.3(8)
N(1)–C(14)–C(13)	112.1(8)	N(5)–C(15)–C(3)	122.7(8)
N(5)–C(15)–C(16)	115.3(9)	C(3)–C(15)–C(16)	121.8(8)
N(6)–C(30)–C(9)	122.8(8)	N(6)–C(30)–C(31)	115.9(8)
C(9)–C(30)–C(31)	121.0(8)		

(14) Stevens, J. C.; Jackson, P. J.; Schammel, W. P.; Christoph, G. G.; Busch, D. H. *J. Am. Chem. Soc.* **1980**, *102*, 3283.

(15) Milazza, G.; Caroli, S. *Tables of Standard Electrode Potentials*; John Wiley: New York, 1978.

(16) Southampton Electrochemistry Group. *Instrumental Methods in Electrochemistry*; Ellis Horwood, Ltd.: Chichester, U.K., 1985.

(17) Chavan, M. Y.; Meade, T. J.; Busch, D. H.; Kuwana, T. *Inorg. Chem.* **1986**, *25*, 314.

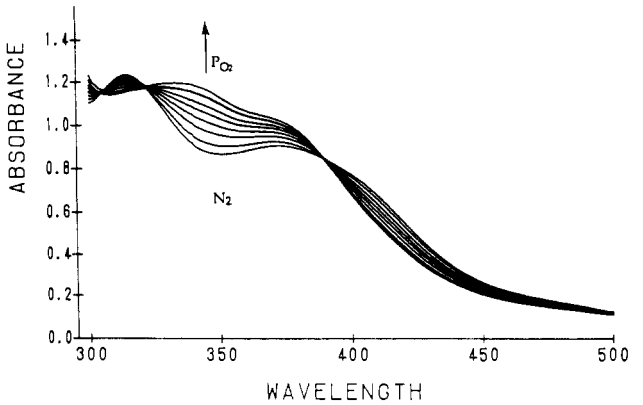

Figure 2. UV–visible spectral changes for $[Co(CH_3)_2(CH_3)_2(CH_2)_9](PF_6)_2$ in 0.15 M 1-methylimidazole/acetonitrile solution at 0 °C, over a range of partial pressures of dioxygen.

Table V. Thermodynamic Properties of Dioxygen Binding to Cobalt(II) Cyclidene Complexes of the Form $Co^{II}(R^3)_2(R^2)_2(R^1)^{2+}$, Where $R^3 = R^2 = CH_3$, in Acetonitrile/0.15 M 1-Methylimidazole

R^1	K_{O_2}, $Torr^{-1}$ (at 0 °C)	ΔH, kcal mol^{-1}	ΔS, eu
$-(CH_2)_6-$[6a,20]	1.32[b]	−17.2	−62
$-(CH_2)_9-$	3.37	−17.1	−60
$-(CH_2)_{10}-$	1.61	−17.4	−63
$-(CH_2)_{11}-$	1.12	−16.1[a]	−59[a]
$-(CH_2)_{12}-$	0.70	−16.9[a]	−63[a]

[a] Results subject to large experimental uncertainty, due to onset of autoxidation within temperature range employed. [b] Measured at 1 °C.

base, such as 1-methylimidazole. The 1-methylimidazole coordinates at the open face of the cobalt(II) cyclidene complex, thus directing the dioxygen-binding process to occur within the cavity. Also, coordination of the cobalt by the axial base increases the electron density on the metal, thereby enhancing the dioxygen affinity. Exposure of a solution of the long-bridged cobalt(II) cyclidene complexes to increasing partial pressures of dioxygen resulted in an increase in absorbance at 305 and 346 nm and a decrease in absorbance at about 410 nm, with isosbestic points at 305 and 390 nm (Figure 2). At low temperature, reversible 1:1 dioxygen binding was observed, and the stoichiometry was confirmed by satisfactory agreement with the Ketelaar equation, which is formulated by assuming a 1:1 stoichiometry.[11] The affinity constants for dioxygen binding were measured at several temperatures, allowing the enthalpy and entropy for dioxygen binding to be determined for these complexes, by means of Van't Hoff plots. These results are summarized in Table V. At higher temperatures, the reversibility of dioxygen binding was impaired by the onset of autoxidation processes. These autoxidation processes are discussed in more detail below. The spectra for $[Co(CH_3)_2(CH_3)_2(CH_2)_9](PF_6)_2$ displayed sharp isosbestic points over the temperature range 0–20 °C. At 25 °C, the isosbestic points were no longer sharp, indicating that the cobalt–oxygen adduct formation is no longer completely reversible. Dioxygen bindings to the $Co(CH_3)_2(CH_3)_2(CH_2)_n(PF_6)_2$ (n = 9–12) complexes were irreversible at 20 and 25 °C, and in the case of the n = 12 complex, the formation of the dioxygen adduct was irreversible at 15 °C. This irreversibility of dioxygen binding to these complexes is exhibited as an increased displacement between the initial UV–visible spectrum under nitrogen and a similar spectrum after the dioxygen-binding experiment. The dependence of the rate of autoxidation on the length of the cyclidene bridge (R^1) is discussed below.

The thermodynamic parameters for dioxygen binding to the long-bridged cobalt(II) cyclidene complexes are similar to those previously reported for other cobalt(II) cyclidene complexes and are shown in Table V. The entropy values are all very similar, which is consistent with this term being dominated by the loss

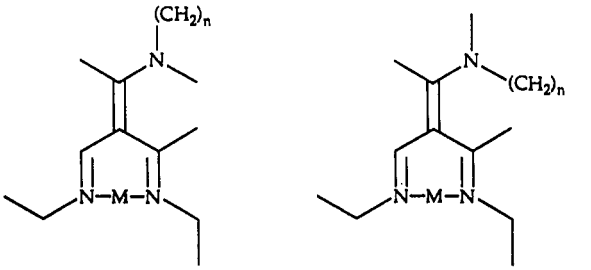

Figure 3. Conformers of bridged cyclidenes: (left) lid-on; (right) lid-off.

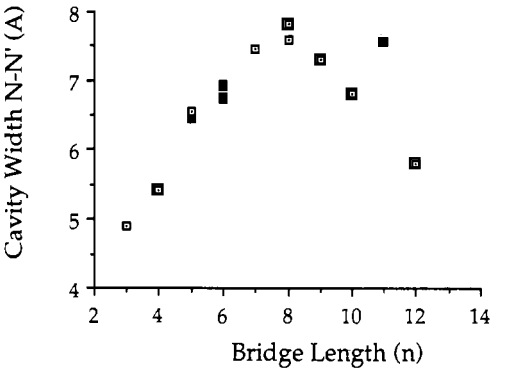

Figure 4. Graph of cyclidene cavity width between bridgehead nitrogens from X-ray diffraction studies. Data are from refs 6c and 7a and this work. Open squares indicate five-coordinate metal (empty cavity); solid squares indicate six-coordinate metal (cavity occupied). Points for two $(CH_2)_6$ empty-cavity structures fall beneath the points for filled-cavity species.

of degrees of freedom of the dioxygen molecule upon coordination to the metal, as previously discussed by Walker.[18] The thermodynamic parameters for the undecamethylene- and dodecamethylene- bridged complexes should only be regarded as estimates, due to the onset of autoxidation within the temperature range used.

Prior to this work, it had been shown that the dioxygen affinity of the $Co(CH_3)_2(CH_3)_2(CH_2)_n^{2+}$ cyclidenes increases systematically with the bridge length over the range n = 4–8. By a combination of techniques, including X-ray diffraction, NMR, and molecular mechanics, the dioxygen affinity has been correlated to the width of the molecular cavity environing the dioxygen-binding site (see Figure 4).[4a,6a,b,d,7a,19] For bridge lengths greater than that of octamethylene, X-ray crystallography, NMR, and molecular mechanics have shown that there is a change in the bridgehead nitrogen conformation, between the so called *lid-off/lid-on* conformations at the bridgehead nitrogen(s) (Figure 3). Switching to the lid-on conformation causes the cavity width to decrease with chain length beyond n = 8, as shown in Figure 4.[6c,7a]

The lid-on/lid-off conformation change is not sharp but is rather a gradual process, with the dodecamethylene-bridged complex having both bridgehead nitrogens in the lid-on conformation, at least in the solid state. In contrast, mixed lid-on/lid-off bridgehead nitrogen conformations are exhibited from the nonamethylene-bridged complex through the undecamethylene-bridged complex.[6c] From this observation, it may be predicted that the dioxygen affinities (K_{O_2}) of the cobalt(II) complexes should systematically decrease on incrementally lengthening the bridge from octamethylene to dodecamethylene. This expectation is borne out by experiment, as shown in a plot of dioxygen affinity (K_{O_2}) against the cobalt(II) cyclidene bridge length (n) (Figure 5). It may be seen that the dioxygen affinity goes through a maximum at n = 8, after which K_{O_2} decreases.

(18) Walker, F. A. *J. Am. Chem. Soc.* **1973**, *95*, 1154.
(19) (a) Meade, T. J.; Fendrick, C. M.; Padolik, P. A.; Cottrell, C. E.; Busch, D. H. *Inorg. Chem.* **1987**, *26*, 4252. (b) Lin, W.-K.; Alcock, N. W.; Busch, D. H. *J. Am. Chem. Soc.* **1991**, *113*, 7603.

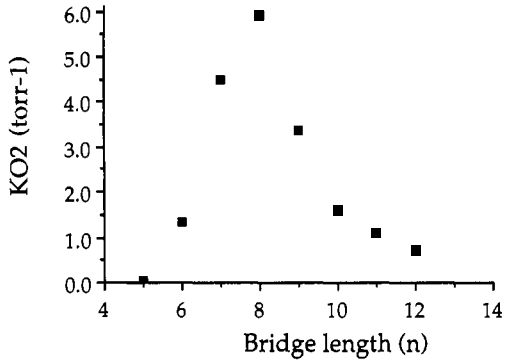

Figure 5. Graph of dioxygen affinity for $Co(CH_3)_2(CH_3)_2(CH_2)_n^{2+}$ complexes in acetonitrile/1.5 M 1-methylimidazole at 0 °C. Data are from refs 20 and 21 and this work.

Crystal Structure of $[Co^{III}(CH_3)_2(CH_3)(CH_2)_{11}(NCS)_2](PF_6)$. As discussed above, there has been a extensive investigation into the parameters which affect the dioxygen-binding process. The cobalt(II) cyclidene complexes are exemplary in this investigation, since the cyclidene is readily derivatized, allowing a systematic comparison of the effects on dioxygen binding that result from ligand substitution. X-ray crystallography has been widely used as a source of quantifiable molecular parameters and, together with molecular mechanics, has been used to examine how the complicated conformation changes that occur upon dioxygen binding are dependent on the bridge length. As discussed above, the dioxygen affinity has been found to be directly correlated to the cavity width, which in turn is dependent on the length of the R^1 polymethylene bridge.[6c,7a] It is therefore of great interest to examine six-coordinate long-bridged complexes. Ideally, it would be preferable to obtain X-ray crystal structures of the dioxygen adducts for comparison; however this approach has not been possible. To date, only one crystal structure is available for the dioxygen adduct of a cobalt(II) cyclidene complex.[20]

Our alternative approach has been to examine the structures of metal complexes coordinated by other small ligands such as carbon monoxide[22] or isothiocyanate.[14,23] Jackson et al. have successfully obtained two crystal structures of bis(isothiocyanato)(cyclidene)cobalt(II), for cyclidenes with $R^1 = -(CH_2)_n-$, $n = 5$ and 6.[14,23] The isothiocyanate ligand coordinated within the cavity has been found to be distorted, in analogy to the bending of carbon monoxide coordinated to hemoglobin. It is therefore of interest to examine the structure of a long-bridged bis(isothiocyanato)(cyclidene)cobalt(III) complex and to compare the results to those for both of the shorter bridged bis(isothiocyanato)cobalt(III) complexes and the longer bridged five-coordinate cyclidene complexes.

The infrared spectrum of $[Co(CH_3)_2(CH_3)_2(CH_2)_{11}(NCS)_2](PF_6)$ in KBr exhibits one band corresponding to the $\nu_{N\equiv C}$ stretching vibration at ca. 2101 cm^{-1}. Previous work with $[Co(CH_3)_2(CH_3)_2(CH_2)_n(NCS)_2](PF_6)$ ($n = 5$–7) revealed two $\nu_{N\equiv C}$ stretches at ca. 2100–2110 and 2032–2045 cm^{-1}, a result that is consistent with the presence of two types of isothiocyanate, one of which is coordinated linearly to the cobalt, outside the cavity, and the other of which is coordinated in a bent manner, within the cavity.[14,23] Since the external isothiocyanate prefers to be coordinated in a linear fashion, any distortion of the internally coordinated isothiocyanate would be expected to result in a different $\nu_{N\equiv C}$ stretching frequency, as has been found for the $Co(CH_3)_2(CH_3)_2(CH_2)_n(NCS)_2^+$ (n = 5–7) complexes. The observation of only one band when $n = 11$ suggests that the cavity is sufficiently large, even after the lid-on/lid-off conformational change, for the degree of bending of the internal thiocyanate ion to be insufficient to differentiate it from the external one, at the IR resolution used for this experiment.

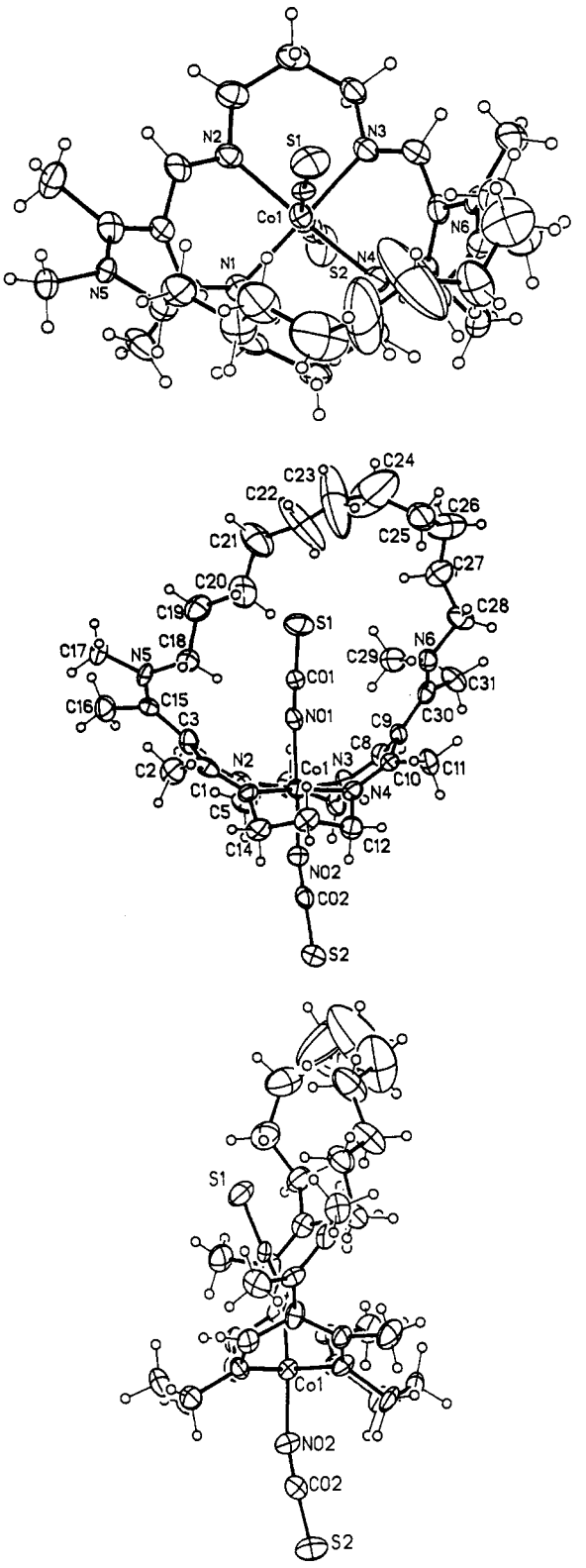

Figure 6. Ortep drawings of $[Co(CH_3)_2(CH_3)_2(CH_2)_{11}(NCS)_2](PF_6)$: (top) view from above; (middle) view looking into cavity; (bottom) view from the side.

X-ray Crystal Structure Analysis. The crystal structure of $[Co(CH_3)_2(CH_3)_2(CH_2)_{11}(NCS)_2](PF_6)$ is shown in Figure 6. The cobalt(III) ion is in a pseudooctahedral environment, and the saturated chelate rings of the N_4 macrocycle adopt chair

(20) Stevens, J. C. Ph.D. Thesis, The Ohio State University, 1979.
(21) Kojima, M.; Busch, D. H. Unpublished results.
(22) Busch, D. H.; Zimmer, L. L.; Grzybowski, J. J.; Olszanski, D. J.; Jackels, S. C.; Callahan, R. C.; Christoph, G. C. *Proc. Natl. Acad. Sci. U.S.A.* **1981**, *78*, 5919.
(23) Jackson, P. J.; Cairns, C.; Lin, W.-K.; Alcock, N. W.; Busch, D. H. *Inorg. Chem.* **1986**, *25*, 4015. Jackson, P. J. Ph.D. Thesis, The Ohio State University, 1981.

Table VI. Comparison of Structural Parameters for Bis(isothiocyanato)(cyclidene)cobalt(III) Complexes with $R^2 = R^3 = CH_3$: Group 1, for SCN Ligand Coordinated within the Cyclidene Cavity; Group 2, for SCN^- Coordinated outside the Cavity

	$-(CH_2)_5-$		$-(CH_2)_6-$		$-(CH_2)_{11}-$	
R^1	1	2	1	2	1	2
Co–N, Å	1.940(4),	1.900(4)	1.94(1)	1.88(1)	1.891(8)	1.881(8)
N–C, Å	1.142(7)	1.173(7)	1.17(1)	1.17(1)	1.158(13)	1.156(14)
C–S, Å	1.617(6)	1.613(6)	1.60(1)	1.60(1)	1.601(10)	1.610(11)
∠Co–N–C, deg	140.8(4)	156.6(5)	148.5(7)	172.3(11)	156.4(7)	166.0(8)
∠N–C–S, deg	178.3(5)	178.8(6)	175.6(10)	174.9(10)	176.6(8)	177.7(9)
ref	23		14		this work	

conformations. The unsaturated rings above the N_4 plane provide the expected saddle-shaped cavity.

As discussed above, crystal structures have previously been obtained for cyclidene complexes containing small molecules bound to the metal, such as carbon monoxide bound to $Fe^{II}(CH_3)_2(H)_2(CH_2)_5^{2+}$ [22] and dioxygen bound to $Co(CH_3)(CH_3)(CH_2)_6^{2+}$,[20] as well as the isothiocyanate anion bound to $Co^{III}(CH_3)_2(CH_3)_2(CH_2)_n^{3+}$ for $n = 5$ and 6.[14,23] The iron (II)–carbon monoxide adduct displayed remarkable distortions of the iron–carbon monoxide bond from the usual linear form due to steric interaction with the cyclidene ligand, attributable to the relatively small cavity produced by the pentamethylene bridge. This effect models the distal steric interactions in the biological heme proteins, suggested as a rationale for their discrimination (compared to simple porphyrins) in favor of dioxygen binding versus carbon monoxide.[24] Of note was the observation that, in the carbon monoxide adduct of the iron cyclidene, the distortion occurred both at the carbon (∠Fe–C–O = 170.6(5)°) and at the iron since the Fe–C bond was displaced 4° from the normal to the N_4 plane.[22] For the cobalt(III) bis(isothiocyanato) complex having the same cavity size, the binding angle of the isothiocyanate anion within the cavity was severely distorted from the expected strain-free linear orientation (∠Co–N–CS = 140.8°), with an accompanying lengthening of the cobalt–NCS bond (1.940 Å), which was 0.04 Å longer than that of the externally coordinated isothiocyanate.[23] The bis(isothiocyanate) complexes of the analogous complex with a hexamethylene bridge and, consequently, larger cavity also exhibited steric interactions involving the internally coordinated thiocyanate. The effect was slightly smaller, with a Co–N–CS angle of 149°, and the internal Co–NCS bond length was again longer (1.92 Å) than that for the external isothiocyanate (1.88 Å).[14,23]

Comparison of the shorter bridged bis(isothiocyanato)(cyclidene)cobalt(III) complexes with the long-bridged complex presented in this work allows clearer identification of the steric control of small-molecule binding within the cyclidene cavity. For the $Co^{III}(CH_3)_2(CH_3)_2(CH_2)_{11}(NCS)_2^+$ complex, the internal isothiocyanate is still slightly distorted from linear coordination, (∠Co–N–CS = 156.4(7)°), presumably because the steric interaction from the hydrogens of the terminal bridge carbons remains significant. In all of these complexes, the primary point of bending of the isothiocyanate is at the nitrogen and the N–C–S angles vary only slightly from 180°.

As was found for the structures of nonamethylene and decamethylene derivatives having empty cavities, the bridge in the new structure has the lid-on conformation on one side and the lid-off conformation on the other. This is the first example in which such a mixed conformation has been observed for a species having a ligand within the cavity. It is interesting that the isothiocyanate is displaced away from the normal to the N_4 plane, toward the side of the complex with the bridgehead nitrogens in the lid-on conformation. Whether this effect is significant remains unclear since there was also a sideways distortion in the analogous pentamethylene complex, for which the lid-off conformation is present on both sides of the structure; this was attributed to crystal packing effects.[23]

The indistinguishability of the SCN infrared stretching frequencies of the internally and externally coordinated isothiocyanates is consistent with the similarity in their cobalt–NCS bond distances and the N–CS bond distances (Table VI), indicating similar strengths of bonding for the two ligands. The externally bound isothiocyanate anion is also significantly bent in this complex (∠Co–N–C = 166.0 (8)°). This is probably the result of a rather short intermolecular contact of 3.316 Å between S(2) and C(4).

Comparison of the structural parameters in Table VI for the undecamethylene-bridged complex with those for its shorter bridged analogues is revealing. Considerable strain is indicated in the pentamethylene- and hexamethylene-bridged complexes, for example, by the difference in the Co–NCS and N–CS bond lengths between the internally and externally coordinated isothiocyanate anions. In contrast, even though there is some steric interaction between the undecamethylene ligand and the internally coordinated isothiocyanate (nonlinear Co–N–C angle), the similarity between the internally and externally coordinated isothiocyanate anions indicates that the bonding of the isothiocyanate to the cobalt(III) metal center is not greatly hindered by the cavity width as has been found for the smaller bridged complexes.

Comparison between the cavity widths (Figure 4) and the dioxygen affinities (Figure 5) shows a clear correlation for both the shorter and longer chains. However, this correlation must arise differently for the two branches of the graphs. For $n \leq 8$, the cavity width is barely altered by the binding of a ligand (filled points in Figure 4; the dioxygen affinity therefore depends on the amount of steric strain caused by interaction between the ligand and the narrow cavity. For the longer chains, the structure reported here shows that the cavity can expand, when a ligand is bound, to a width close to the optimum value in the series (that for $n = 8$). The decrease in dioxygen affinity as the chain length increases ($n = 8$–12) must therefore arise from the energy barrier for this expansion, as a combination of the energy needed to distort the cyclidene unit and that to reorient the chain. The magnitude of the effect on dioxygen affinities is similar on the two sides of the graph so that the affinities for long-chain complexes with a particular cavity width are only slightly larger than those for the corresponding short-chain complexes.

Autoxidation of the Long-Bridged Cobalt(II) Cyclidenes. In common with all known dioxygen carriers, the long-bridged cobalt(II) cyclidene complexes undergo autoxidation in solution. This process is conveniently defined as irreversible oxidation, occurring in the presence of dioxygen, which is in addition to the reversible dioxygen-binding process. Although the autoxidation processes have only been fully characterized for relatively few dioxygen carriers, it is clear that there are several different types of mechanisms. Further details about the autoxidation of dioxygen carriers, both the biological heme proteins and synthetic model compounds, may be found in a recent review.[25] The

(24) Collman, J. P.; Brauman, J. I.; Doxsee, K. M. *Proc. Natl. Acad. Sci. U.S.A.* **1979**, *76*, 6035.

(25) Warburton, P. R.; Busch, D. H. In *Perspectives in Bioinorganic Chemistry*; Hay, R. W., Ed.; JAI Press: London, in press.

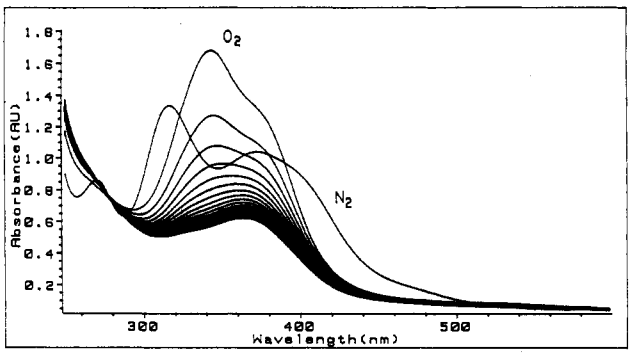

Figure 7. UV–visible spectrum of $Co(CH_3)_2(CH_3)_2(CH_2)_{11}(PF_6)_2$ in acetonitrile containing 0.15 M 1-methylimidazole at 25 °C, showing initial spectrum under nitrogen, spectra after exposure to dioxygen (760 Torr) for 2 min, and thereafter at ten min intervals.

Table VII. Pseudo-First-Order Rate Constants for the Autoxidation of Cobalt(II) Cyclidene Complexes of the Form $[Co(R^3)_2(R^2)_2(R^1)](PF_6)_2$, Where $R^3 = R^2 = CH_3$, in Acetonitrile/1.5 M 1-Methylimidazole, at 25 °C, Saturated with 760 Torr of Dioxygen

R^1	rate, s^{-1}	R^1	rate, s^{-1}
$-(CH_2)_6-$[26]	$(3.0 \pm 0.3) \times 10^{-4}$	$-(CH_2)_{11}-$	$(3.0 \pm 0.6) \times 10^{-3}$
$-(CH_2)_9-$	$(1.5 \pm 0.3) \times 10^{-3}$	$-(CH_2)_{12}-$	$(5 \pm 1) \times 10^{-3}$
$-(CH_2)_{10}-$	$(2.0 \pm 0.4) \times 10^{-3}$		

application of dioxygen carriers is limited by their lifetime in the presence of dioxygen. Therefore, it is important to elucidate the autoxidation process, if conditions are to be found under which these degradation reactions are to be controlled.

Solutions of the long-chain cobalt(II) cyclidene complexes of the general form $Co(CH_3)_2(CH_3)_2(CH_2)_n(PF_6)_2$ (n = 9–12) in acetonitrile, containing an excess of 1-methylimidazole, are found to undergo autoxidation in the presence of dioxygen. The autoxidation process can be observed in the decay of the ESR signal due to the oxygen adduct ($g_\perp = 2.016$, $g_\parallel = 2.091$)[4a] and may conveniently be followed by UV–visible spectroscopy, as shown in Figure 7, as a decay either of the cobalt(II) bands (λ_{max} = 320 and 376 nm) or of the dioxygen adduct bands (λ_{max} = 350 nm), depending on the partial pressure of dioxygen. From the kinetics of the process, it is apparent that at least two reactions are involved. This conclusion is confirmed on examining the UV–visible spectral changes with time, from which it is apparent that two processes are occurring, rather than one process, with a more complex rate law. The kinetics may be satisfactorily fitted to two consecutive first-order rate equations. The rate of autoxidation dictates the lifetime of a dioxygen carrier in any given application, and thus the parameters of the fastest autoxidation process are of most interest, and these will be expanded in more detail below.

Of particular note to this communication is the observation that the rate of autoxidation exhibits only a gentle increase on varying the length of the bridging group from n = 5 to n = 8.[27] In contrast, the rate of autoxidation increases dramatically on increasing n from 9 to 12, as shown in Table VII. This greatly enhanced propensity toward autoxidation is probably a consequence of the lid-on/lid-off transformation occurring on lengthening the bridging group though the mechanism of this effect remains unclear.

It is of interest to examine how the autoxidation mechanism for the complexes with longer bridges compares to that for the shorter bridged analogs. A plot of observed rate of autoxidation

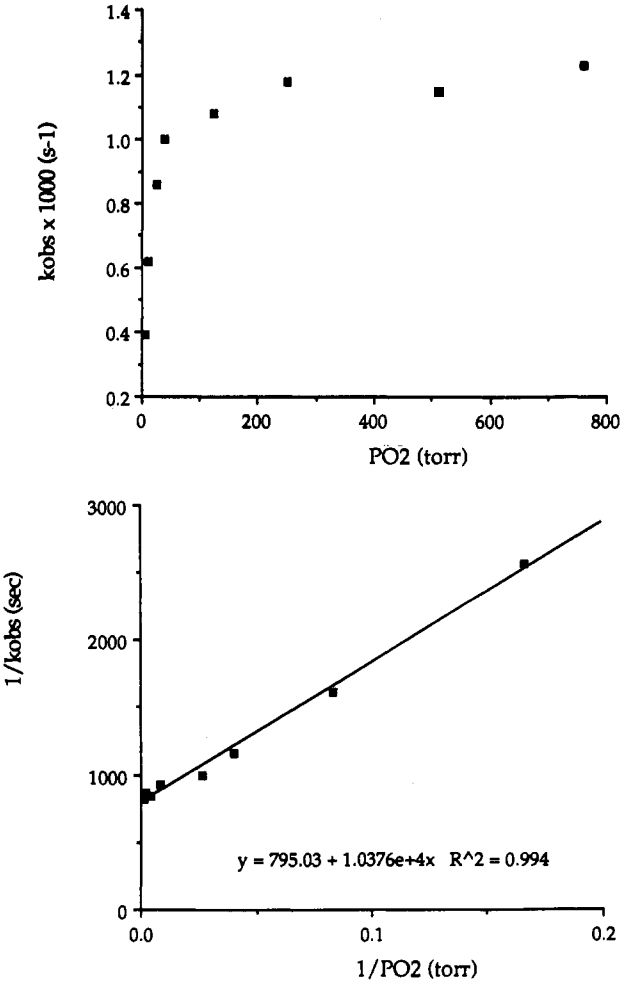

Figure 8. (Top) Graph of the pseudo-first-order rate of autoxidation of $[Co(CH_3)_2(CH_3)_2(CH_2)_{11}](PF_6)_2$ in acetonitrile containing 0.15 M 1-methylimidazole over a range of partial pressures of dioxygen at 30 °C. (Bottom) Graph of the inverse of the pseudo-first-order rate constant of autoxidation versus the inverse of the partial pressure of dioxygen.

of the $Co(CH_3)_2(CH_3)_2(CH_2)_{11}(PF_6)_2$ complex in acetonitrile containing excess 1-methylimidazole versus the partial pressure of dioxygen exhibits a nearly linear dependence at low partial pressures of dioxygen, but it shows saturation behavior for higher partial pressures of dioxygen. A plot of the inverse of the observed rate versus the inverse of the partial pressure of dioxygen is linear (Figure 8). From the equations describing a kinetic process with a preequilibrium,[26] the equilibrium constant of the preceding chemical equilibrium may be obtained by dividing the intercept by the slope of this line. The mathematical forms of the rate laws are similar whether the autoxidation reaction is competitive with or consecutive to dioxygen binding.

$$CoLB + O_2 \leftrightarrow CoL(O_2)B \quad (K_{O_2})$$

(i) consecutive reaction: $CoL(O_2)B \rightarrow$ products (k)

$$\text{obs rate} = kK_{O_2}[CoL][O_2]/(1 + K_{O_2}[O_2])$$

(ii) competitive reaction: $CoLB + O_2 \rightarrow$ products (k')

$$\text{obs rate} = k'[CoL][O_2]/(1 + K_{O_2}[O_2])$$

This equilibrium process probably corresponds to the formation of the dioxygen adduct, and this assignment is confirmed by the similarity of the equilibrium constant derived from the rates of

(26) Espenson, J. H. *Chemical Kinetics and Reaction Mechanisms*; McGraw-Hill: New York, 1981.
(27) Masarwa, M.; Warburton, P. R.; Evans, W. E.; Busch, D. H. *Inorg. Chem.*, submitted for publication.
(28) *CRC Handbook of Chemistry and Physics*; Weast, R. C., Astle, M. J., Eds.; CRC Press: Boca Raton, FL, 1966–67.

Table VIII. Rate of Autoxidation of $[Co(CH_3)_2(CH_3)_2(CH_2)_{11}](PF_6)_2$ in Acetonitrile/0.15 M Base, Saturated with Dioxygen, at 25 °C, Measured at 350 nm

base	pK_b of base at 25 °C[28]	obs rate of autoxidn, s^{-1}
acetonitrile		0.64×10^{-4}
pyridine	5.25	2.9×10^{-4}
1-methylimidazole	6.95	7.5×10^{-4}
diisopropylamine	10.96 (28.5 °C)	1.7×10^{-3}
tributylamine		1.7×10^{-3}

autoxidation (K_{O_2} = 0.08 $Torr^{-1}$, 30 °C) to the separately determined K_{O_2} of this complex under similar conditions (K_{O_2} = 0.06 $Torr^{-1}$, 30 °C; extrapolated value from equilibrium measurements). Similar agreement was found for the dodecamethylene- bridged complex (K_{O_2} from autoxidation = 0.06 $Torr^{-1}$, K_{O_2} extrapolated from equilibrium measurements = 0.03 $Torr^{-1}$, 30 °C). A similar dependence of the rate of autoxidation on the partial pressure of dioxygen was found for the shorter bridged cobalt(II) cyclidene complexes.[27]

There is considerable evidence that the first step of the autoxidation of the shorter bridged cobalt(II) complexes of this series involves a deprotonation of the cyclidene ligand at the R^3 position, prior to an oxidation step.[27] In order to examine whether the same mechanism is rate-determining in the autoxidation of the long-bridged $Co(CH_3)_2(CH_3)_2(CH_2)_n(PF_6)_2$ complexes, the effects of the basicity of the axial base and the axial base concentration were investigated. The rates of autoxidation of $Co(CH_3)_2(CH_3)_2(CH_2)_{12}(PF_6)_2$ were measured in acetonitrile containing a range of bases, and the results are presented in Table VIII. The rates are significantly enhanced in the presence of stronger bases. For strong bases such as diisopropylamine, the reaction was completed in too short a time to permit accurate rate constant measurements under these experimental conditions. The enhancement of the autoxidation rate in the presence of stronger bases indicates that the rate-determining step of the autoxidation process for the long-bridged cobalt(II) cyclidene complexes is associated with deprotonation, as for the shorter bridged complexes.

The rate of autoxidation increases with temperature, as would be expected. From the slope of a graph of ln k_{obs} versus $1/T$, the activation energy for the autoxidation process was calculated to be 73 K J mol^{-1} for $[Co(CH_3)_2(CH_3)_2(CH_2)_{11}](PF_6)_2$ in acetonitrile containing 1.5 M 1-methylimidazole, under 1 atm of dioxygen. A more complete discussion of the mechanism of the autoxidation of cobalt(II) cyclidene complexes and the characterization of the products will be presented elsewhere.[27]

Acknowledgment. The financial support of the National Science Foundation is gratefully acknowledged. Dr. Tho. Nguyen of the University of Kansas supplied some of the elemental analyses and Dr. Todd Williams and Mr. Bob Drake, also of the Univerity of Kansas, supplied the mass spectral measurements. These contributions are deeply appreciated.

Supplementary Material Available: Listings of anisotropic thermal parameters, full bond lengths and angles, and H atom coordinates (4 pages). Ordering information is given on any current masthead page.